



C. S. Huang
X. Q. Liu
Y. R. Chen

Facial asymmetry index in normal young adults

Authors' affiliations:

C. S. Huang, Faculty of Dentistry, Craniofacial Research Center, Chang Gung Memorial Hospital, Taipei, Taiwan
C. S. Huang, Y. R. Chen, Graduate Institute of Dental & Craniofacial Science, Chang Gung University, Taoyuan, Taiwan
X. Q. Liu, Department of Orthodontics, The Affiliated Hospital of Medical College, Qingdao University, Qingdao, Shandong Province, China
Y. R. Chen, Department of Plastic Surgery, Craniofacial Research Center, Chang Gung Memorial Hospital, Taipei, Taiwan

Correspondence to:

Chiung S. Huang
Chang Gung Craniofacial Research Center
Chang Gung Memorial Hospital
199 Tunghwa North Road
Taipei
Taiwan
E-mail: sshuang@ms1.hinet.net

Huang C. S., Liu X. Q., Chen Y. R. Facial asymmetry index in normal young adults

Orthod Craniofac Res 2013; **16**: 97–104. © 2012 John Wiley & Sons A/S. Published by Blackwell Publishing Ltd

Structured Abstract

Objectives – To differentiate a symmetric face from an asymmetric face by analyzing a three-dimensional (3D) facial image and plotting the asymmetry index (AI) on a facial symmetry diagram.

Setting and Sample Population – Sixty healthy Chinese adults (30 men and 30 women, mean age: 27.7 + 4.9 years old) without any craniofacial deformity were recruited on a voluntary basis from a medical center.

Material and Methods – A 3D facial image of each participant was captured by a GENEX 3D FACE CAM system. Sixteen facial landmarks, as defined by Farkas, were selected on each 3D facial image. The AI was calculated for each landmark.

Results – The norm for the AI varied from 0.76 to 2.82. The landmarks located on the upper face had a smaller AI than the landmarks located on the lower face. A facial symmetry diagram was designed according to the mean, one standard deviation, and 2 standard deviations of AI for each landmark.

Conclusions – The 3D facial asymmetry can be documented with AI. The landmarks located on the upper face had a smaller AI than the landmarks located on the lower face. The facial symmetry diagram can identify efficiently the location of asymmetry on a face.

Key words: asymmetry index; facial asymmetry; facial symmetry diagram; surface scan; three-dimensional facial image

Introduction

Facial asymmetry is a three-dimensional (3D) problem that is common in patients with dentofacial deformity (1–5). Traditionally, two-dimensional (2D) cephalometric radiography (e.g., lateral and postero-anterior views) was commonly used to evaluate facial symmetry (1, 6). However, it is difficult, and impossible, to

Date:

Accepted 3 November 2012

DOI: 10.1111/ocr.12009

© 2012 John Wiley & Sons A/S. Published by Blackwell Publishing Ltd

evaluate 3D craniofacial structures with 2D cephalometry (7, 8), in addition to the concern of radiation haphazard. Recently, clinical evaluation of craniofacial deformities became available with the introduction of a non-invasive 3D surface image technique (9–15). Faces can be viewed from various angles with accurate measurements in length, angle, area, and volume by using a non-invasive 3D surface imaging technique. In clinical practice, it is crucial to differentiate an asymmetric face from a symmetric face. A face is basically a symmetric structure in regard to right and left (3, 16, 17). It is crucial to first determine the factors that constitute a normal face and the extent of deviation that can be allowed in a normal face before further consideration of orthodontic or combined orthodontic and orthognathic treatments. A 3D surface image of a facial coordinate system was established to evaluate facial symmetry in adults that appeared to have symmetrical faces. The primary goal of this study was to delineate the degree of facial asymmetry that can be allowed in a so-called normal face. A facial symmetry diagram was designed to delineate the asymmetric range allowed in a normal face for each anatomical facial landmark.

Material and methods

Participants

A group of 60 healthy Chinese adults without any craniofacial deformity were recruited on a voluntary basis from a medical center, and included 30 men and 30 women, aged 20–35 years, with a mean age of 27.7 ± 4.9 years (mean \pm SD). The participants were selected according to the following criteria:

- Dental occlusion Angle Class I.
- No craniofacial deformity.
- No facial trauma history.
- No prior orthodontic or orthognathic surgery.
- Face regarded as normal symmetry by an orthodontist, a plastic surgeon, and a nurse.

Informed consent was obtained from each participant before the face scan.

Three-dimensional face scan

The 3D facial images were captured with the GENEX 3D FACE CAM System (Genex Technologies, Inc. Kensington, MD, USA). The scan time for a face was 400 ms. During the scan, the participants sat comfortably in a cushioned chair with back support, and their heads were maintained in a natural head position. The use of spectacles or earrings was not allowed during the scan. All image data were processed by a personal computer to generate a surface model suitable for subsequent visualization and analysis by custom-designed software (Beauty 3D, V1.5; Logistic Technology, Taoyuan, Taiwan).

The 16 facial landmarks, as defined by Farkas (18), were selected on the 3D facial images (Table 1). The landmarks were digitized on the computer screen by an experienced operator (XQL), and the *x*, *y*, and *z* coordinates were recorded. As shown in Fig. 1, the midfacial plane (*yz* plane) was determined by a plane passing through the nasion and perpendicular to the transverse plane (*xy* plane) connecting the nasion

Table 1. The definition and abbreviation of sixteen landmarks, defined by Farkas (18)

Landmarks	Abbr.	Definition
Glabella	Gla	Most prominent midline point between eyebrows
Nasion	Na	Deepest point of nasal bridge
Pronasale	Prn	Most protruded point of the apex nasi
Subnasale	Sn	Midpoint of angle at columella base
Labial superius	Ls	Midpoint of the upper vermilion line
Stomion	Sto	Midpoint of the mouth orifice
Labial inferius	Li	Midpoint of the lower vermilion line
Menton	Me	Most inferior point on chin
Exocanthion*	Exc	Outer commissure of the eye fissure
Endocanthion*	End	Inner commissure of the eye fissure
Alar curvature*	Ala	Most lateral point on alar contour
Cheilion*	Ch	Point located at lateral labial commissure

The landmarks indicated with * are paired landmarks, those without * are midline landmarks.

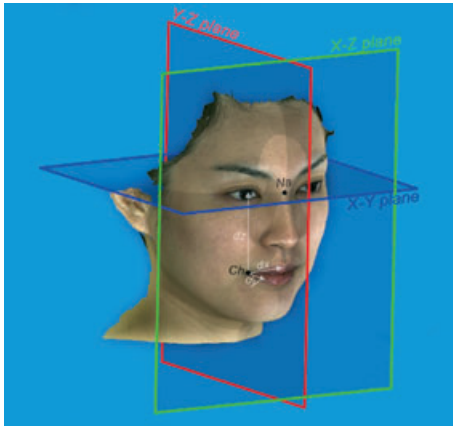


Fig. 1. Three-dimensional (3D) reference planes (i.e., xy plane, xz plane, and yz plane) shown on a three-quarter view of a 3D face scan image. Point of right cheilion illustrates the linear measurements of dx, dy, and dz to each respective plane.

and bilateral exocanthion. The coronal plane was defined as the xz plane perpendicular to the midfacial plane and passing through the nasion. The transverse plane was defined as xy plane perpendicular to the midfacial plane and the coronal plane and passing through the nasion. Each landmark can be assessed by zoom-in, translation, and rotation movements of the surface model to ensure accurate 3D location of landmarks.

To evaluate facial asymmetry, the distances of each landmark to three reference planes were measured as dx, dy, and dz in millimeters (Fig. 1). The values of dx, dy, and dz of the nasion were zero. For each paired bilateral landmark, the differences in dx, dy, and dz between the right side and left side indicated the discrepancy of the paired landmarks in three dimensions. For perfect symmetrical paired bilateral landmarks, the discrepancy in dx, dy, and dz must approach zero. No difference must occur between dy and dz values between the right and left side for the facial midline landmarks located on the midfacial plane, and dx represents the discrepancy from the facial midline. To evaluate facial symmetry, an asymmetry index (AI): $AI = \sqrt{(Ldx - Rdx)^2 + (Ldy - Rdy)^2 + (Ldz - Rdz)^2}$ was calculated for each landmark, where L = left and R = right.

Intra-observer error in identifying each landmark was conducted on 10 randomly selected samples at 2-week intervals using the following formula: $D = \sqrt{(\Delta x)^2 + (\Delta y)^2 + (\Delta z)^2}$, where D is

Table 2. Asymmetry index of landmarks in normal adults (n = 60)

Landmarks	Abbr.	Mean	SD	Max	Min
Glabella	Gla	0.76	0.59	3.28	0.03
Pronasale	Prn	0.88	0.68	2.78	0.04
Subnasale	Sn	0.78	0.55	2.16	0.02
Labial superius	Ls	0.86	0.70	3.05	0.02
Stomion	Sto	0.98	0.75	3.28	0.06
Labial inferius	Li	1.19	0.80	3.05	0.06
Menton	Me	1.54	1.50	6.40	0.06
Exocanthion	Exc	1.00	0.62	3.04	0.32
Endocanthion	End	1.21	0.57	2.65	0.22
Alar curvature	Ala	2.33	1.07	4.88	0.62
Cheilion	Ch	2.82	1.42	6.50	0.40

All units are in mm.

Asymmetry index (AI) was measured using formula: $AI = \sqrt{(Ldx - Rdx)^2 + (Ldy - Rdy)^2 + (Ldz - Rdz)^2}$, L: left, R: right.

the total error for each landmark, Δx is the difference in the X coordinate, Δy is the difference in the Y coordinate, and Δz is the difference in the Z coordinate.

Results

Intra-observer errors in identifying landmarks ranged from 0.31 to 0.95 mm, with a mean of 0.52 mm. Table 2 shows the norm for the AI in 60 participants. The mean AI varied from 0.76 to 2.82, with a standard deviation (SD) from 0.42 to 1.50. For the midline landmarks, AI exhibited greater variation in the lower face, compared to those in the upper face. Point menton in the lower midface exhibited the largest AI (1.54 ± 1.50), whereas glabella in the upper face exhibited the smallest AI (0.76 ± 0.59). The bilateral landmarks also demonstrated a similar tendency with greater AI and more variation in the lower face (i.e., cheilion: 2.82 ± 1.42) and smaller AI and less variation in the upper face (i.e., exocanthion: 1.00 ± 0.62). Figure 2 shows a diagram to indicate the mean and standard deviation (SD) of AI for each landmark. The mean and SD are represented in light green and green, respectively, for normal variation. The deviation from

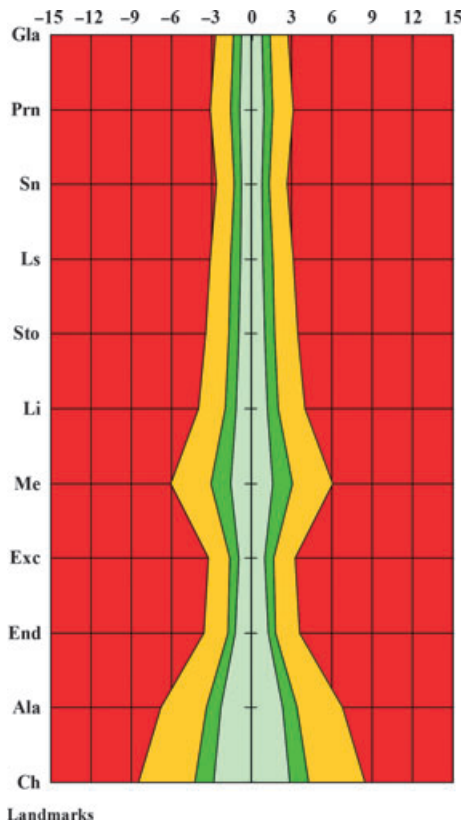


Fig. 2. Facial soft tissue asymmetry indices in normal adults. A visual graphic diagram represents the mean and standard deviation (SD) of asymmetry indices of each facial landmark on participants. In frontal view, if $Ldx - Rdx$ is a negative value, the landmark deviates more toward the right. If $Ldx - Rdx$ is a positive value, the landmark deviates more toward the left. The light green zone represents the range of asymmetry index mean for all facial landmarks. The $Ldx - Rdx$ value determines the plot of each landmark on the positive or negative range. For each landmark, the green area represents symmetry with deviation of <1 SD. The yellow area represents asymmetry area with deviation of more than 1 SD, but <2 SD. The red area represents marked asymmetry area with the deviation of more than 2 SD.

one SD to 2 SD for each landmark is defined as asymmetry and is represented in yellow. The deviation from more than 2 SDs is defined as marked asymmetry and is represented in red. This facial symmetry diagram was used to evaluate the degree of facial asymmetry for each participant.

Figure 3 shows a 3D surface scan of a 24-year-old man with a repaired left unilateral complete cleft lip and palate. Marked asymmetry is presented in the alar curvature, cheilion, and menton. Figure 4 shows the AI value of each landmark plotted on a normal AI symmetry diagram. The blue line represents the AI value for the patients. The current clinical evaluation of



Fig. 3. Three-dimensional surface scan of 24-year-old man with repaired complete cleft lip and palate. Red dots indicate the locations of 16 landmarks.

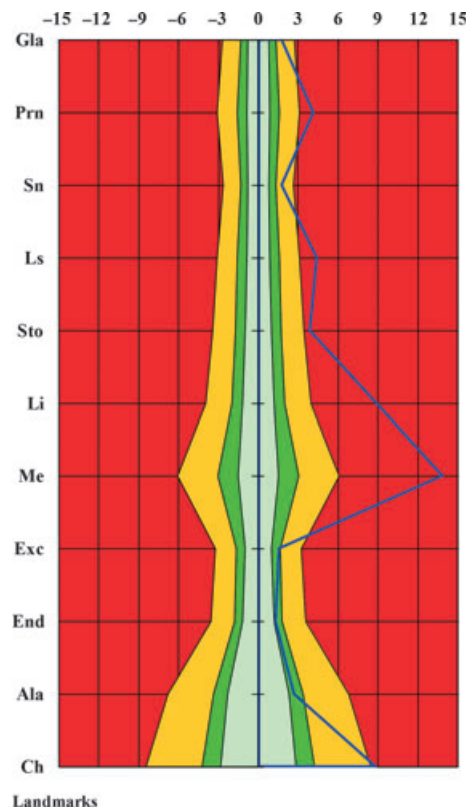


Fig. 4. The asymmetry index values plotted on a facial symmetry diagram. Marked asymmetry was identified for those landmarks located in the red zone. Right- and left-side deviation was determined by dx value. For each landmark, dx value was calculated by subtracting x coordinate on left with x coordinate on right. The positive dx value indicates that the landmark deviates toward the left, and the negative dx value indicates that the landmark deviates toward the right.

facial asymmetry is mainly based on the discrepancy located in the x coordinate for each landmark. For each landmark, the value of dx represents the subtraction of the left x coordinate from the right x coordinate. The positive dx value indicates that the deviation is more toward the left side, and vice versa.

Discussion

Perfect symmetry in the bilateral body is a theoretical concept that is rarely observed in real-world biology (16). Slight facial asymmetry is a common biological variation in 'normal' humans (17). A midfacial plane must be determined first to assess facial asymmetry accurately. The proper selection of the midfacial plane is the crucial step in the clinical evaluation of facial asymmetry. For 2D cephalometric analysis, the midfacial plane can be constructed by two or three midsagittal landmarks (19, 20). If three midsagittal landmarks are used, these three landmarks are often not located in a straight line. Vig and Hewitt (1) noted the difficulty in drawing a straight line connecting sella, anterior nasal spine, and the midpoint between right and left orbitals. Therefore, they used the best-fit line of these three anatomical landmarks to represent the midline of the face. For a 3D coordinate system, the midfacial plane can be formed by three points located at facial midline structures (21, 22). However, the midfacial plane constructed by three reference point-based internal midline structures of the skull (e.g., sella, basion, and opisthion) may differ from the midfacial plane constructed by three reference points based on the external midline structure (e.g., nasion, anterior nasal spine, and menton) (23, 24). For clinical evaluation, the midfacial plane must be closely related to the external facial structures, as perceived by patients and clinicians. Reconfirmation of the chosen midfacial plane on real patients is possible if these reference points are located on external facial structures. In addition to the location of these three reference points on external facial structures, they must be separated as widely as possible to include the whole

dimension of the face, and can also be used to reconstruct three reference planes (i.e., midfacial plane, coronal plane, and axial plane) simultaneously. Therefore, several researchers (4, 20, 23, 25) chose a midfacial plane perpendicular to the line that connects bilateral external facial or skeletal landmarks. Ras et al. (20) used stereophotogrammetry to assess 90 participants without craniofacial anomalies. They compared four reference planes perpendicular to the bilateral exocanthion, endocanthion, superalare, and cheilion. They concluded that the optimal reference plane to assess 3D facial asymmetry is the plane perpendicular to and bisecting the line that connects the bilateral exocanthion. However, the point bisecting the bilateral exocanthion line may differ from the location of midfacial landmarks (e.g., nasion) in the x coordinate. For clinical application, a number of studies (4, 23, 25) indicated that it is preferable to choose the midfacial plane passing through the nasion and perpendicular to the plane connecting the two exocanthions and nasion. In this study, the midfacial plane was defined by the plane passing through nasion and perpendicular to the bilateral exocanthions. Soft tissue nasion is located at a distinctly depressed area directly between the eyes and slightly above the bridge of the nose. The reproducibility of point nasion is usually superior to other anatomical facial landmarks. In the frontal view, soft tissue nasion is usually located at the intersection of medially extended bilateral eyebrows. Exocanthion is located at the outer corner of the eye fissure at which the eyelids meet. The bilateral exocanthion is separated by a large distance that can reduce the effect of a slight error derived from landmark identification. Most maxillofacial surgeries are usually performed below eye level. The reference plane using both exocanthions can be used for superimposition between pre- and post-operative facial images.

The AI was first proposed by Katsumata et al. (19) for the assessment of facial asymmetry in 3D CT images. However, they did not differentiate the right- or left-side deviation for each landmark because of a small sample size. The AI on a 3D CT was modified and applied to a 3D facial

surface scan analysis in this study. The right–left asymmetry in the x coordinate is crucial in clinical treatment because it is easier to detect by patients when they look into a mirror from the frontal view. Right–left discrepancy must be delineated first in the clinical evaluation of facial asymmetry. A facial symmetry diagram was designed for clinicians to easily identify the location of facial asymmetry. The dx value of each landmark represents the deviation in the x coordinate from the midfacial plane. The positive dx value indicated more deviation toward the left, and vice versa. By plotting the AI value for each landmark, facial asymmetry can be clearly represented in the facial symmetry diagram. The clinician can immediately detect the location of the asymmetry, and further 3D analysis can be performed for the component of facial asymmetry in the x , y , and z coordinates. Because nasion is used to reconstruct the axial plane and midfacial plane, the AI value for nasion must be zero. The random error in identifying nasion is in the range of 0.31–0.95 mm. The position of nasion must be validated first to reconstruct a clinical and meaningful midfacial plane. Furthermore, the position of nasion may be distorted due to nasofrontal trauma or in craniofacial anomalies. The location of nasion must be feasible to construct the midfacial plane before further AI analysis is performed.

The results of our study show that facial asymmetry is more obvious when moving downward on the face. Similar findings have been reported in several previous studies (18, 20, 26–28). Farkas (18) found that the facial asymmetry that occurs in normal people is lower than 2% for the eye and orbital region, lower than 7% for the nasal region, and approximately 12% for the oral region. The greatest asymmetry identified in this study was located at the cheilion, with a mean and SD of 2.82 ± 1.42 mm, respectively. This finding is consistent with that of Farkas and Cheung (17), who stated that facial asymmetry, if <3 mm or 3% of right–left difference, is indiscernible in a normal face. Peck et al. (28) analyzed 52 well-balanced Caucasian adult faces for skeletal asymmetry using a posteroanterior cephalogram. They concluded that the means

and ranges of deviation were 0.87 mm, 0–4 mm at the laterosuperior orbit, 2.25 mm, 0–9 mm at the lateral zygoma, and 3.54 mm, 0–12 mm at the gonion, respectively. Less asymmetry and more dimensional stability were observed as the cranium was approached. The difference between right and left laterosuperior orbital can be as large as 4 mm without the appearance of facial asymmetry. The location and laterosuperior orbit on the bone corresponds to the exocanthion on skin. The maximal tolerance of asymmetry at the exocanthion was 3.04 mm in normal adults in this study. For normal adults, the asymmetry between bilateral orbital cavities must not be >3.0 mm at soft tissue and 4.0 mm at hard tissue. Ras et al. (20) used stereophotogrammetry to assess facial asymmetry in 90 participants without craniofacial anomalies and found that the difference was greater for the bilateral landmarks from cranial to caudal (e.g., exocanthion, alare, and cheilion). Katsumata et al. (19) used 3D CT to assess 16 patients whose 3D CT scans were assessed by three radiologists with the impression of no craniofacial asymmetry. The AI for midline skeletal and dental landmarks was greater when moving from the upper face to lower face. The AI values for the anterior nasal spine, upper central incisor, lower central incisor, and menton were 0.8, .0.9, 1.2, and 1.8, respectively. For the corresponding points on soft tissue, the AI values identified in this study for the subnasale, labial superior, labial inferior, and menton were 0.78, 0.86, 1.19, and 1.54, respectively. A greater variation in facial asymmetry was identified in both hard and soft tissue landmarks when moving from the upper to lower face. Greater asymmetry can be allowed in lower faces of adults with normal appearance. The maximal asymmetry allowed in the menton and cheilion can be as high as 6.50 mm.

The limitations of this study are as follows: All participants were Chinese. Various ethnic groups must be included to delineate the range of variation in the AI value. All participants were recruited from a medical center. Therefore, this sample may not represent the whole population. The speed of facial scan was relatively slow

(400 ms per scan). Facial asymmetry can only be evaluated under a static position without any dynamic movement (e.g., smiling and speech). Functional facial movement must be studied with higher-speed facial scanning in the future. The number of participants in this study was insufficient to detect sex differences in facial asymmetry. An increase in the number of participants of both sexes may be required in future studies to differentiate the role of sex in affecting the AI value. For this study, the age range was limited to 20–35 years. The age range can be expanded to include younger and older adults. A facial scan of soft tissue must be matched with a hard tissue scan (e.g., computerized tomography) to study the correlation between soft tissue symmetry and hard tissue symmetry.

Facial asymmetry is common in so-called normal faces. The AI using the formula $AI = \sqrt{(Ldx - Rdx)^2 + (Ldy - Rdy)^2 + (Ldz - Rdz)^2}$ was proposed and delineated on 16 facial landmarks. The landmarks located on the upper face exhib-

ited smaller AI, compared to the landmarks located on the lower face. The facial symmetry diagram can efficiently identify the location of the asymmetry on the right or left side of the face.

Clinical relevance

Facial asymmetry is a biological variation that commonly occurs in humans. It is crucial for clinicians to differentiate a symmetrical face from an asymmetrical face. A 3D facial surface scan can be used to establish an asymmetric index for each facial landmark. The AI can be plotted on a facial symmetry diagram to delineate the part of the face that is asymmetric.

Acknowledgements: This study was supported by grants from the National Science Council (NSC 97-2314-B-182-020-MY2) and Chang Gung Memorial Hospital (CMRPG 370231, 381631). The authors would like to thank Ms. MF Lin for the manuscript and graphic preparations.

References

- Vig PS, Hewitt AB. Asymmetry of the human facial skeleton. *Angle Orthod* 1975;45:125–9.
- Haraguchi S, Iguchi Y, Takada K. Asymmetry of the face in orthodontic patients. *Angle Orthod* 2008;78:421–6.
- Severt TR, Proffit WR. The prevalence of facial asymmetry in the dentofacial deformities population at the University of North Carolina. *Int J Adult Orthodon Orthognath Surg* 1997;12:171–6.
- Plooij JM, Swennen GR, Rangel FA, Maal TJ, Schutyser FA, Bronkhorst EM et al. Evaluation of reproducibility and reliability of 3D soft tissue analysis using 3D stereophotogrammetry. *Int J Oral Maxillofac Surg* 2009;38:267–73.
- Al-Omari I, Millett DT, Ayoub AF. Methods of assessment of cleft-related facial deformity: a review. *Cleft Palate Craniofac J* 2005;42:145–56.
- Grayson BH, McCarthy JG, Bookstein F. Analysis of craniofacial asymmetry by multiplane cephalometry. *Am J Orthod* 1983;84:217–24.
- Gateno J, Xia JJ, Teichgraber JF. New 3-dimensional cephalometric analysis for orthognathic surgery. *J Oral Maxillofac Surg* 2011;69:606–22.
- Gateno J, Xia JJ, Teichgraber JF. Effect of facial asymmetry on 2-dimensional and 3-dimensional cephalometric measurements. *J Oral Maxillofac Surg* 2011;69:655–62.
- Weinberg SM, Naidoo S, Govier DP, Martin RA, Kane AA, Marazita ML. Anthropometric precision and accuracy of digital three-dimensional photogrammetry: comparing the Genex and 3dMD imaging systems with one another and with direct anthropometry. *J Craniofac Surg* 2006;17:477–83.
- Weinberg SM, Scott NM, Neiswanger K, Brandon CA, Marazita ML. Digital three-dimensional photogrammetry: evaluation of anthropometric precision and accuracy using a Genex 3D camera system. *Cleft Palate Craniofac J* 2004;41:507–18.
- Ghoddousi H, Edler R, Haers P, Wertheim D, Greenhill D. Comparison of three methods of facial measurement. *Int J Oral Maxillofac Surg* 2007;36:250–8.
- Sforza C, Laino A, D'Alessio R, Dellavia C, Grandi G, Ferrario VF. Three-dimensional facial morphometry of attractive children and normal children in the deciduous and early mixed dentition. *Angle Orthod* 2007;77:1025–33.
- Khambay B, Nairn N, Bell A, Miller J, Bowman A, Ayoub AF. Validation and reproducibility of a high-resolution three-dimensional facial imaging system. *Br J Oral Maxillofac Surg* 2008;46:27–32.
- Sawyer AR, See M, Nduka C. 3D stereophotogrammetry quantitative lip analysis. *Aesthetic Plast Surg* 2009;33:497–504.
- Toma AM, Zhurov A, Playle R, Ong E, Richmond S. Reproducibility of facial soft tissue landmarks on 3D laser-scanned facial images. *Orthod Craniofac Res* 2009;12:33–42.
- Bishara SE, Burkey PS, Kharouf JG. Dental and facial asymmetries: a review. *Angle Orthod* 1994;64:89–98.
- Farkas LG, Cheung G. Facial asymmetry in healthy North American Caucasians. An anthropometrical study. *Angle Orthod* 1981;51:70–7.

18. Farkas LG. *Anthropometry of the Head and Face*, 2nd edn. New York: Raven Press Ltd; 1994.
19. Katsumata A, Fujishita M, Maeda M, Ariji Y, Ariji E, Langlais RP. 3D-CT evaluation of facial asymmetry. *Oral Surg Oral Med Oral Pathol Oral Radiol Endod* 2005;99:212–20.
20. Ras F, Habets LL, van Ginkel FC, Prahl-Andersen B. Method for quantifying facial asymmetry in three dimensions using stereophotogrammetry. *Angle Orthod* 1995; 65:233–9.
21. Baek SH, Cho IS, Chang YI, Kim MJ. Skeletodental factors affecting chin point deviation in female patients with class III malocclusion and facial asymmetry: a three-dimensional analysis using computed tomography. *Oral Surg Oral Med Oral Pathol Oral Radiol Endod* 2007;104:628–39.
22. Kwon TG, Park HS, Ryoo HM, Lee SH. A comparison of craniofacial morphology in patients with and without facial asymmetry—a three-dimensional analysis with computed tomography. *Int J Oral Maxillofac Surg* 2006;35:43–8.
23. Damstra J, Fourie Z, De Wit M, Ren Y. A three-dimensional comparison of a morphometric and conventional cephalometric midsagittal planes for craniofacial asymmetry. *Clin Oral Investig* 2012;16:285–94.
24. Hajeer MY, Ayoub AF, Millett DT. Three-dimensional assessment of facial soft-tissue asymmetry before and after orthognathic surgery. *Br J Oral Maxillofac Surg* 2004;42:396–404.
25. de Menezes M, Rosati R, Ferrario VF, Sforza C. Accuracy and reproducibility of a 3-dimensional stereophotogrammetric imaging system. *J Oral Maxillofac Surg* 2010;68: 2129–35.
26. Ferrario VF, Sforza C, Miani A, Tartaglia G. Craniofacial morphometry by photographic evaluations. *Am J Orthod Dentofacial Orthop* 1993;103:327–37.
27. Ferrario VF, Sforza C, Miani A Jr, Serrao G. A three-dimensional evaluation of human facial asymmetry. *J Anat* 1995;186(Pt 1):103–10.
28. Peck S, Peck L, Kataja M. Skeletal asymmetry in esthetically pleasing faces. *Angle Orthod* 1991;61:43–8.

Copyright of Orthodontics & Craniofacial Research is the property of Wiley-Blackwell and its content may not be copied or emailed to multiple sites or posted to a listserv without the copyright holder's express written permission. However, users may print, download, or email articles for individual use.